Vol. 01, Iss. 1 (2023) 21-25, DOI: 10.61552/JME.2023.01.003

JME

Journal of Materials and Engineering

www.jme.aspur.rs

Research article

Effect of Cross-Sectional Profile of Circular Dimples on Hydrodynamic Lubrication Characteristics of Thrust Bearings

Ryota Ishii[a], Reo Miwa[a], Norifumi Miyanaga[a,*], Jun Tomioka[b]

[a]*Kanto Gakuin University, Yokohama, Japan,*
[b]*Waseda University, Tokyo, Japan.*

Keywords:

Thrust bearings
Hydrodynamic lubrication
Dimples
Load-carrying capacity
Frictional torque

* Corresponding author:

Norifumi Miyanaga
E-mail: miyanaga@kanto-gakuin.ac.jp

Received: 15 March 2023
Revised: 14 April 2023
Accepted: 24 April 2023

A B S T R A C T

The effects of three types of dimples with different internal structures on the fluid lubrication characteristics of thrust bearings were investigated. The load-carrying capacity and the frictional torque were measured. The measurements were performed with a fixed constant film thickness. The behaviours of cavitation bubbles occurred within the dimple were observed through the rotating glass plate. Three types of internal structures of dimples were tested: cylindrical, sphere and conical. The measurement results were simulated by the Reynolds equation. As the results, the load-carrying capacity increased as the rotational speed increased. The cylindrical internal structure built up the largest pressure at the trailing edge, and consequently the largest load-carrying capacity. The frictional torque also increased with increasing the rotational speed. However, the effect of the internal structure on the frictional torque was not significant.

© 2023 Journal of Materials and Engineering

1. INTRODUCTION

Since the pioneering works by Etsion et al. [1], texturing has attracted attention as a means of improving the lubrication performance of machine elements. The effect of the internal structures of dimples has not been sufficiently studied, despite its importance in determining the hydrodynamic lubrication characteristics. It is notable that Shen et al. [2] experimentally and numerically studied the effect of several dimple internal shapes on the load-carrying capacity. Nanbu et al. [3] numerically studied the EHL performance for different dimple bottom shapes.

In this study, the effects of different internal structures of dimples on the lubrication characteristics were investigated. The load-carrying capacity (LCC) and the frictional torque were measured with a fixed constant oil film thickness. The behaviors of cavitation bubbles in dimples were also observed. The experimental results were discussed with analytical results.

2. EXPERIMENTS

Fig. 1 shows a schematic of the experimental apparatus used in this study [4-5]. The thrust bearing consists of an upper glass disk and a dimpled brass specimen. The disk rotates in unison with a rotating shaft, which is supported by an aerostatic bearing. The dimpled specimen is fixed in an oil cup. A Peltier device is built in the bottom of the oil cup to maintain lubricant temperature constant. Unlike conventional tribometers in which a constant load is applied to bearings, this apparatus controls the oil film thickness and is able to measure the load-carrying capacity by a normal force sensor located in the measuring head. The frictional torque can be also measured by a torque sensor. The lubricated surface can be observed through a glass disk. To improve the visibility, a green laser is irradiated in the form of a sheet.

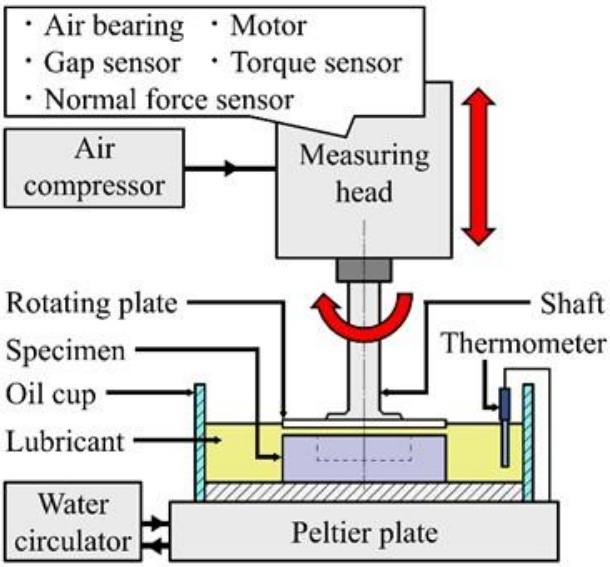


Fig. 1. Experimental apparatus.

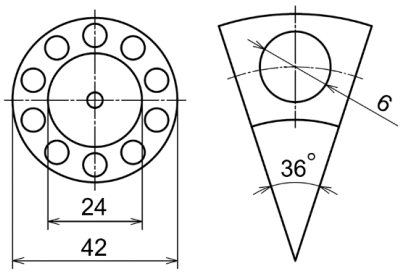


Fig. 2. Specimen and dimple dimensions.

Fig. 2 shows a schematic of dimpled specimens whereas Fig. 3 shows internal structures of tested specimens. The inner and outer diameters of the lubricating surface were d_o=42mm and d_i=24mm, respectively. Ten dimples with the diameter of d_d=6mm were evenly located on the lubricating surface of the specimens. Three types of internal structures were tested: cylindrical, sphere and conical. Each dimple was drilled to be the maximum depth of approximately δ_{max}=30μm. For each dimple, the area ratio of the dimple to the lubricating surface was 30%.

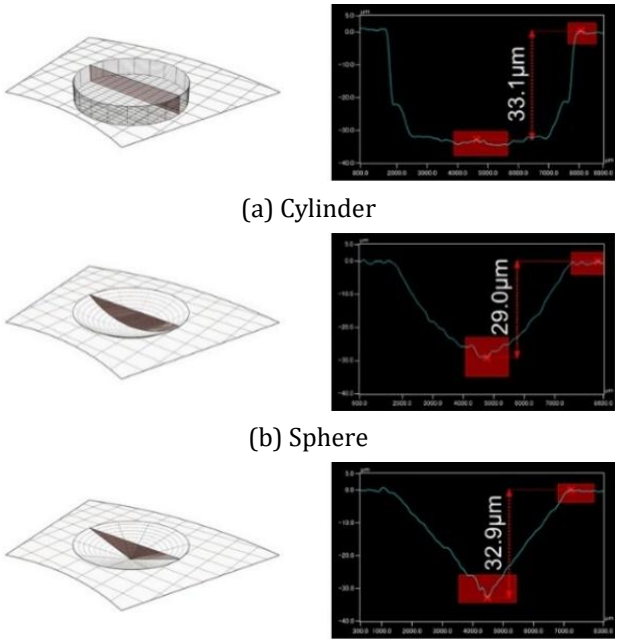


Fig. 3. Internal structures of the tested dimples: (a) cylindrical, (b) spherical and (c) conical.

3. NUMERICAL ANALYSIS

The experiments were simulated to explain the test results for three types of the internal structures of the dimples. The Reynolds equation for the r-θ coordinate, formula (1), was used for calculations.

$$\frac{\partial}{\partial r}\left(rh^3\frac{\partial p}{\partial r}\right)+\frac{\partial}{\partial \theta}\left(\frac{h^3}{r}\frac{\partial p}{\partial \theta}\right)=6r\frac{\partial h}{\partial \theta} \quad (1)$$

where p is the oil film pressure. An analytical model with a single dimple is shown in Fig. 4. This model corresponds to the part of one-tenth of the bearings. Selecting a cavitation pressure is problematic when cavitation in dimpled bearings is numerically treated. In this study, the half-Sommerfeld condition was adopted, basing on the works of Etsion et al. [1]. In addition, the atmospheric pressure was assumed at the radial bearing ends and the cyclic conditions were for the circumferential ends.

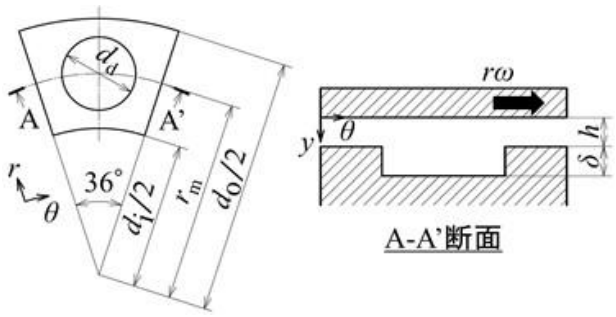


Fig. 4. Single dimple model for analysis.

4. RESULTS AND DISCUSSION

4.1 Experimental results

Fig. 5 shows the measurement results of the frictional torque for each dimple. In the measurements, the oil film thickness was set to h=30μm. The error bar indicates the standard deviation. The plane is the result for the dimple-free bearing whose theoretical result can be calculated by formula (2).

$$T = \frac{\pi\eta\omega(d_o{}^4 - d_i{}^4)}{32h} \quad (2)$$

where T is the frictional torque, h is the fixed constant oil film thickness, η is the viscosity of lubricant, ω is the angular velocity. The experimental frictional torque of the dimple-free specimen agreed with the theoretical value, which valid that the oil film thickness was properly controlled.

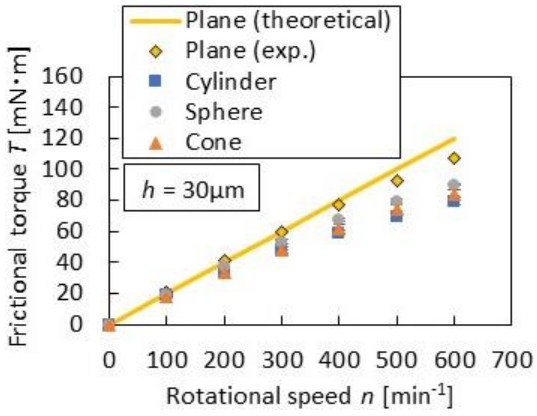


Fig. 5. Measurement results of frictional torque.

For all dimples, the frictional torque increased with increasing rotational speed. The frictional torque of the dimpled bearings were reduced, compared to that of the dimple-free bearing. The effect of the internal structure of the dimples was not significant. It is considered that the frictional force was dominated by the ridge-part, which occupy 70% of the sliding surface. The cylindrical dimple demonstrated the lowest frictional torque.

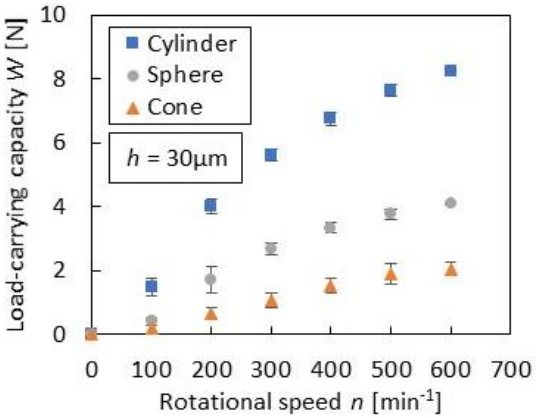


Fig. 6. Measurement results of LCC.

Fig. 6 shows the relationship between the LCC and the rotational speed. In this measurement, the oil film thickness was regulated so as to be h=30 μm. Error bars indicate the standard deviation. The LCC increased with increasing the rotational speed, regardless of the internal structure. With comparing the three dimples, the cylindrical dimple had the largest load-carrying capacity whereas the cone had the smallest valuse. Within the scope of this study, the maximum LCC of the cylindrical dimples was approximately four times greater than that of the conical dimples. The effect of the internal structures on the LCC is quite remarkable.

Fig. 7 compares the observed results of cavitation bubbles generated in the dimples at the rotation speed of n=600 min^{-1}. The arrows in the figure indicate the rotational direction of the glass disk. Cavitation bubbles were generated within the dimples. The seat-shaped cavitation bubbles were observed in the cylindrical dimples whereas the finger-shaped bubbles were observed in the conical and sphere dimples.



a) Cylinder b) Sphere



c) Cone

Fig. 7. Cavitation bubbles in dimples (600min^{-1}).

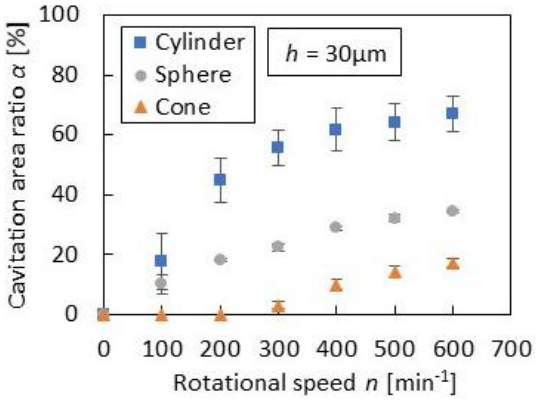


Fig. 8. Estimated results of cavitation area ratio.

Fig. 8 shows the results of the cavitation area ratio. The ratio α was calculated by formula (3).

$$\alpha = \frac{A_c}{A_d} \times 100 \qquad (3)$$

where A_d and A_c are the areas of the dimple and the cavitation bubble, respectively.

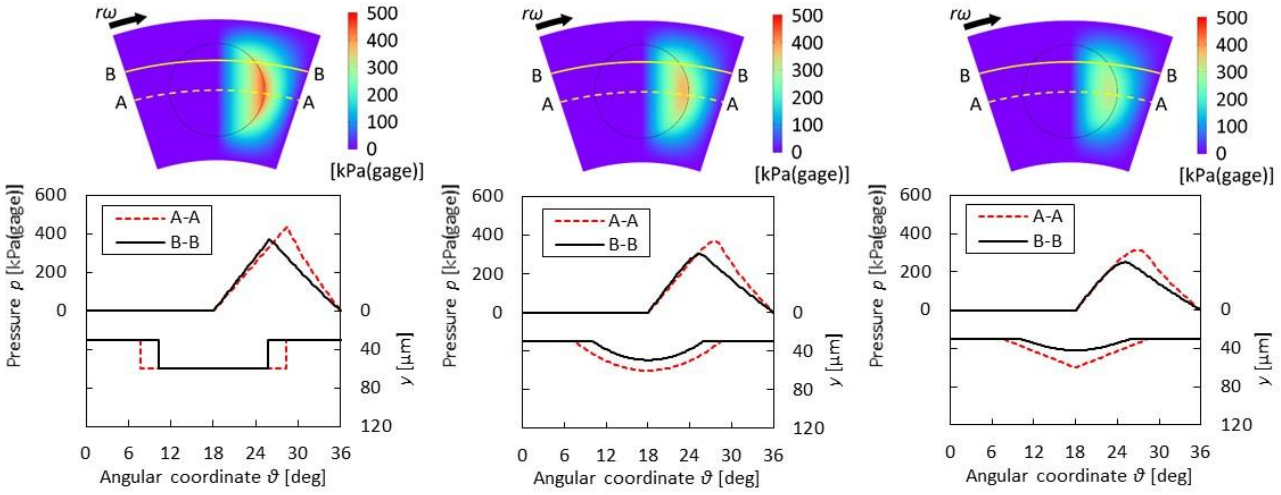
The cavitation area ratio α was the largest in the cylindrical dimple, and it reached more than 60% as the rotational speed increased. It would be concluded that for the conical dimple, the cavitation area ratio α was quite small at n=100 and 200 min^{-1}, and therefore the LCC shown in Fig. 7 was also small.

4.2 Analytical results

Fig. 9 shows the analytical pressure contours, and 2D distributions in A-A (r=r_m) and B-B (r=r_m+Δr) sections. The arrow indicates the rotating direction of the smooth glass plate.

The cylindrical dimple had the highest pressure whereas the cone had the lowest. These results are consistent with the experimental results, in which the cylindrical dimple had the largest LCC. The pressure reached the maximum value on the trailing edge for the cylindrical dimple whereas slightly inside for the sphere and cone dimples. In addition, in the sphere and cone dimples, the peaks of pressure are not sharp compared to that in the cylindrical dimple.

For sphere and cone dimples, the wedge effect is not sufficient since the dimple depth gradually shallows as Δr increases. It would be large impact to the difference in LCC for each dimple internal structure.



(a) Cylinder (b) Sphere (c) Cone

Fig. 9. Analytical pressure distribution for each internal structure.

5. CONCLUSIONS

The effects of the internal structures of dimples on the lubrication characteristics were investigated. The cylindrical internal structure indicated both the largest LCC and the lowest frictional torque. The shape of cavitation bubbles was different in different internal structures.

REFERENCES

[1] I. Etsion and L. Burstein, "A model for mechanical seals with regular microsurface structure," *Tribology Transactions*, vol. 39, no. 3, pp. 677–683, 1996, doi: 10.1080/10402009608983582.

[2] C. Shen and M. M. Khonsari, "Effect of dimple's internal structure on hydrodynamic lubrication," *Tribology Letters*, vol. 52, no. 3, pp. 415–430, 2013, doi: 10.1007/s11249-013-0225-8.

[3] T. Nanbu, T. Ren, Y. Yasuda, D. Zhu, and Q. J. Wang, "Micro-textures in concentrated conformal-contact lubrication: Effects of texture bottom shape and surface relative motion," *Tribology Letters*, vol. 29, no. 3, pp. 241–252, 2008.

[4] N. Miyanaga, T. Kishida, and J. Tomioka, "Experimental investigation of load-carrying capacity and frictional torque of dimpled parallel thrust bearings," *Journal of Advanced Mechanical Design, Systems, and Manufacturing*, vol. 14, no. 3, article no. JAMDSM0041, 2020.

[5] R. Miwa, N. Miyanaga, and J. Tomioka, "Appearance of hysteresis phenomena on hydrodynamic lubrication in a seal-type thrust bearing with dimples," *Materials*, vol. 14, no. 18, article no. 5222, 2021, doi: 10.3390/ma14185222.